S.-Afr.Tydskr.Geol.1988,91(1)38–48

Sedimentary facies of the Dwyka Formation associated with the Nooitgedacht glacial pavements, Barkly West District

J.N.J. Visser and J.C. Loock

Department of Geology, University of the Orange Free State, P.O. Box 339, Bloemfontein 9300, Republic of South Africa

Received 10 November 1987

Lithofacies of the Dwyka Formation associated with the Permo-Carboniferous glacial pavements and representing the national monument on Nooitgedacht 66, Barkly West District, include, bouldery diamictite (facies 1); coarse, clast-rich diamictite (facies 2A and 2B); bedded, fine, clast-rich diamictite (facies 3); stratified, fine, clast-rich diamictite (facies 4); conglomerate (facies 5), and mudrock (facies 6). Facies 1, 2B, and 3 form part of drumlinoid complexes, facies 2A and 4 occur in floor lows, facies 5 is found along the flank of a bedrock knob, and facies 6 overlaps the diamictites onto the Ventersdorp Supergroup basement. Facies 1 and 2B formed subglacially in leeside cavities by expulsion of stones from the ice roof of the cavity and by *in situ* melt-out of debris-rich basal ice. Facies 2A has a probable lodgement origin, whereas facies 3 formed by melt-out of slivers of stagnant debris-rich basal ice lodged on the stoss-sides of bedrock knobs. Facies 4 represents predominantly debris-flow deposits. Conglomerate facies 5 formed by the reworking of diamicton by meltwater streams in subglacial tunnels and cavities. The mudrocks of facies 6 accumulated by suspension settling of mud from turbid plumes, rain-out of ice-rafted debris, and deposition by debris flows and turbidites. Analysis of the subglacial deposits and erosional features suggests low mean normal stresses at the ice-bedrock interface, a fairly low sliding velocity for the basal ice, low basal meltwater pressures, and an ice thickness of probably more than a 100 m. Deposition took place during the final disintegration stage when the ice flowed into a water body which covered the area.

Litofasies van die Dwykaformasie, geassosieerd met die Perm-Karboongletservloere wat tot 'n nasionale monument op Nooitgedacht 66, Barkly-wes-distrik, verklaar is, sluit rolblokdiamiktiet (fasies 1); growwe, klasryke diamiktiet (fasies 2A en 2B); gelaagde, fyn, klasryke diamiktiet (fasies 3); meerlagige, fyn, klasryke diamiktiet (fasies 4); konglomeraat (fasies 5), en moddergesteentes (fasies 6) in. Fasies 1, 2B, en 3 vorm deel van drumlinvormige komplekse, fasies 2A en 4 kom in lae gedeeltes in die vloer voor, fasies 5 is langs die flank van 'n vloerbult aangetref, en fasies 6 oorvleuel al die diamiktieteenhede tot op die vloergesteentes van die Supergroep Ventersdorp. Fasies 1 en 2B het in subglasiale lykantholtes deur die ontsetting van klaste vanuit die ysdak van die holte en uitsmelting in plek van puinbelaaide basale ys, gevorm. Fasies 2A het 'n moontlike smeeroorsprong, terwyl fasies 3 deur die uitsmelting van stagnante, puinbelaaide, basale ysstroke wat aan die stootkant van vloerbulte vasgesteek het, ontstaan het. Fasies 4 verteenwoordig hoofsaaklik puinvloei-afsettings. Konglomeraatfasies 5 het deur die herwerking van diamikton deur smeltwaterstrome in subglasiale tonnels en holtes gevorm. Die moddergesteentes van fasies 6 het deur suspensie-uitval van modder vanuit modderige pluime, uitreën van dryfyspuin en afsetting vanuit puinvloeie en turbidiete ontstaan. Ontleding van die subglasiale afsettings en die erosiestrukture dui op lae gemiddelde druktoestande op die vlak tussen die ys en die vloergesteentes, 'n redelike lae glysnelheid vir die basale ys, lae basale smeltwaterdrukke en 'n ysdikte van moontlik meer as 100 m. Afsetting het gedurende die finale disintegrasiefase toe die ys in 'n watermassa oor die hele gebied ingevloei het, plaasgevind.

Introduction

The glacial pavements that developed during the Permo-Carboniferous glaciation on the farm Nooitgedacht 66, about 20 km northwest of Kimberley, were declared a national monument in 1936. These pavements are easily reached, being about 6 km along a gravel road from the Kimberley – Barkly West tarred road. The exposures occur on the eastern side of a large meander in the Vaal River, known as 'The Bend', and were probably first referred to by Du Toit in 1906.

The pavements drew renewed attention after a visit to the area by a group during the International Geological Congress in 1929. Since then detailed descriptions of the glacial erosion features have been published (Slater, 1932; Stratten, 1968; Engelbrecht, 1973), but very little has appeared on the glacial deposits associated with the pavements. It is essential that these rock types are described in detail as they form an integral part of the national monument. The objectives in this paper are therefore:

(i) a facies analysis of the diamictites, conglomerates and mudrocks deposited by the ice in the area,
(ii) to describe their mode of deposition, and
(iii) to define the characteristics of the ice forming the outstanding glacial features.

Altogether 24 individual pavements, which consist of lava of the Ventersdorp Supergroup, have been recorded on Nooitgedacht 66 (Engelbrecht, 1973). This study was however confined to three pavements within about 400 m from the old homestead and to good exposures in a stream-bed to the east of the homestead (Figure 1). The basement outcrops consist of polished and striated dome-like rock knobs (length:width ratio = 1) with fairly steep (up to 35°) stoss-sides and gentle leesides mostly covered by glacial debris (Figure 2). The glacial erosion features therefore do not comply to the definition of roche moutonnées (knobs of bedrock with gently inclined stoss-sides, steep and rough leesides, and long axes orientated in the direction of ice flow) and can best be defined as drumlinoid complexes with a rock

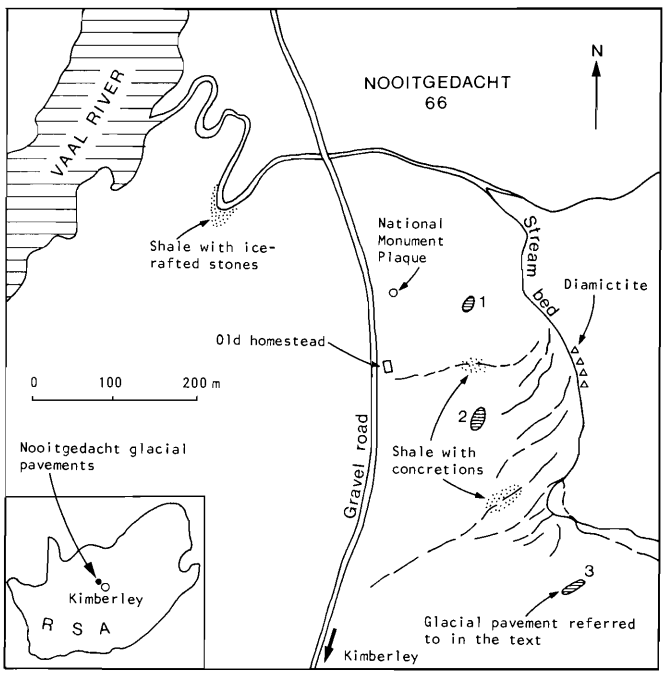

Figure 1 Locality map showing the glacial pavements, the gullies, and the stream-bed where diamictites, conglomerate, and mudrocks were studied on Nooitgedacht 66.

nucleus and a tail of glaciated debris. The term 'crag and tail' is commonly used for such features, whereas Eyles & Menzies (1983) applied the term 'drumlinoid bedrock-drift complexes' for diamicton units wedging out against bedrock highs, coupled with scree-like leeside accumulations. The easternmost pavement however, occurring topographically several metres above the other, show smoothly abraded 'whalebacks' with diamictite preserved in between the cigar-shaped polished outcrops.

For descriptive purposes the pavements studied were numbered 1 to 3 (Figure 1) and, except for pavement 3, they occur in fenced-in areas. As this is a national monument no stones were removed, and the facies analyses were therefore based on short stratigraphic sections and the orientation of the clast a-axes. The high dips of the stoss-side beds also influenced the decision of the authors to record only the long axes of the clasts. Lastly, as it is exclusively glacial rocks that are dealt with in this paper, no data is given on the glacial pavements or the ice-flow directions. Readers interested in these aspects are referred to the reports by Slater (1932) and Engelbrecht (1973).

Lithofacies descriptions

In the description of Slater (1932) on the sedimentary exposures at Nooitgedacht, Slater (1932) distinguished only between tillite and varved shale, whereas Engelbrecht (1973) described, in addition to the tillites and varved shales, a thin bed of fine-grained, laminated material directly overlying the pavements. Both Slater (1932) and Stratten (1968) mentioned the presence of grooves on top of diamictite near the old homestead.

In this study a lithofacies approach based on the texture, which includes clast-packing density (CPD), structure, and fabric of the rocks was used. Four diamictite facies, including two subfacies, were defined. In addition to these a conglomerate and a mudrock facies were also present. In the statistical analysis of the a-axis orientation of the clasts the Von Mises distribution (Till, 1974) was used. Values for r (an estimate of the angular values around a unit circle and which can be represented by a mean resultant length) and k (concentration parameter; the higher the k-value the greater the preferred orientation) were also calculated.

Facies 1 (bouldery diamictite)

The facies occurs as longitudinal median ridges on the leesides of pavements 1 and 2. The ridges are up to 35 m long and 5 m wide, have a matrix to clast-supported

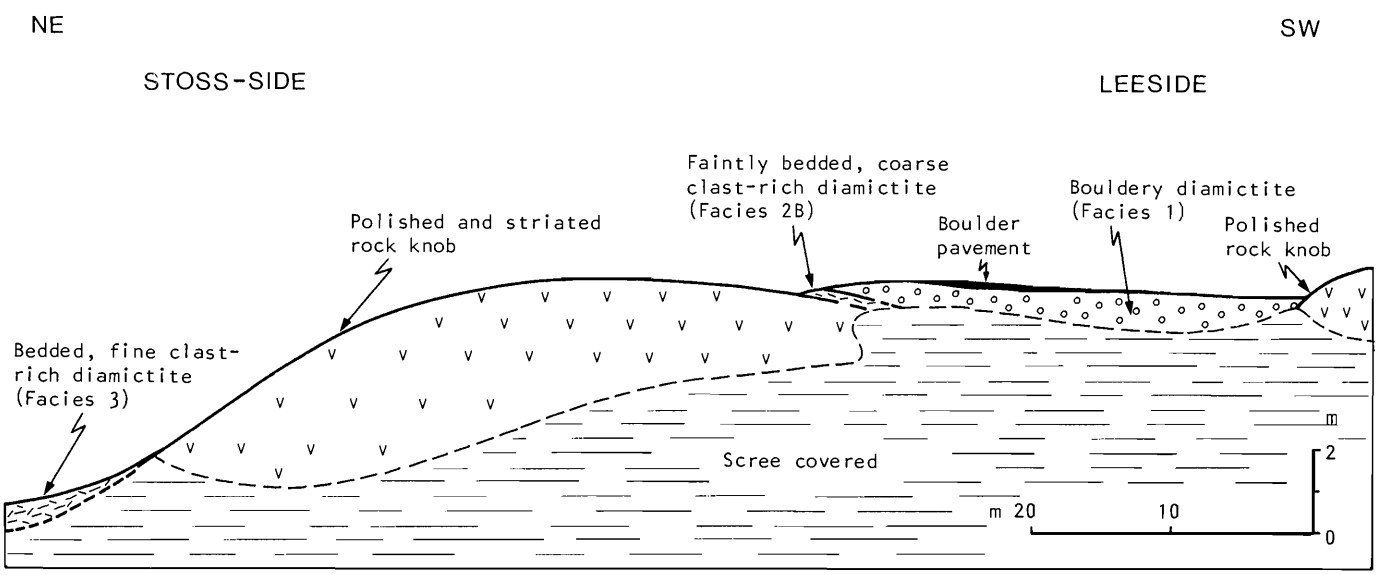

Figure 2 Northeast-southwest section across pavement 1 showing the drumlinoid complex consisting of a bedrock nucleus with stoss- and leeside diamictites.

Figure 3 Bouldery diamictite of facies 1 consisting of densely packed clasts [Ventersdorp lava clast (Vd) is 1,2 m long] with abraded tops. The surface may represent a boulder pavement. Ice flow indicated by an open arrow.

texture, and consist of large (up to 1,7 m in length), rounded clasts in an argillaceous to arenaceous matrix (Figure 3). The facies has a thickness of about 1 m (Figure 4) and at the northeastern ends of the pavements overlies clast-rich diamictite of facies 2B. Almost 50 per cent of the clasts show striations. The top of the boulder ridge at pavement 1 is abraded with striations being parallel to the strike of the ridge which suggests a possible boulder pavement (Figure 3). The clast a-axes show preferred orientations with k-values between 1,5 and 2 (Figure 5).

Facies 2 (coarse clast-rich diamictite)

The coarse clast-rich diamictite facies occurs on the leesides of, or in lows between, bedrock knobs (Figure 6). It consists of fairly densely packed (CPD = 23–26%), matrix- supported, rounded to subrounded clasts which are up to 80 cm in diameter. The matrix consists of about 20 per cent angular to subrounded sand and silt-sized fragments, mostly of quartz, feldspar, lava, granite, quartzite, and mudrock in dark-brown ferruginous to argillaceous material. The thickness of the facies probably does not exceed 2 m. The facies rests directly on lava of the Ventersdorp Supergroup (Figures 2 and 4) and is in turn overlain by the bouldery diamictite of facies 1 or stratified diamictite of facies 4 (Figures 4 and 7).

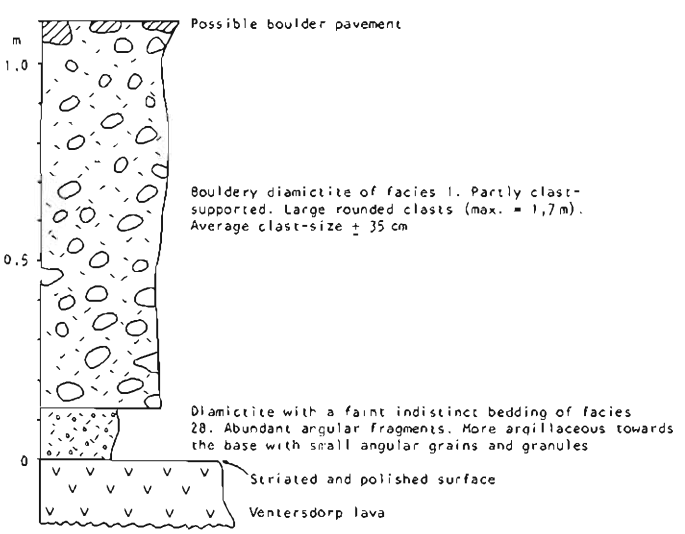

Figure 4 Stratigraphic section of leeside diamictite (facies 1 and 2B) at pavement 1.

Subfacies 2A, which is exposed in the stream-bed, is apparently massive (Figure 7) and the clasts have good a-axis orientations with k-values > 4 (Figure 5). The diamictite surface contains grooves which are covered by a mudrock drape (Figure 8). The orientation of the grooves is parallel to the regional ice-flow direction (220°–230°). Subfacies 2B which occurs on the leesides of pavements 1 and 2, varies from apparently massive to faintly bedded (Figure 9). The bedding, where noticeable, consists of very indistinct planes in the diamictite. The clasts show very poor a-axis orientations with k-values between 1 and 1,5 (Figure 5).

Facies 3 (bedded, fine, clast-rich diamictite)

This diamictite facies occurs on the stoss-sides of bedrock knobs where it has a maximum thickness of about 0,6 m. It consists of angular to subrounded dispersed (CPD = 16%) clasts (up to 30 cm in diameter), in an argillaceous to silty matrix. At pavement 2 an outsize clast truncates the distinct bedding (Figure 10) which consists of alternating mudrock, sandy and granular layers (Figure 11). Bed contacts are commonly deformed and partly diffused. A few small mudstone clasts are also present. The stones show very poor a-axis orientations with k-values between 1,3 and 1,5 (Figure 5). Engelbrecht (1973) also reported secondary modes in the orientation of the clasts and this results in the deviation of the clast long axes by about 45° from the general ice-flow direction. At pavement 2 the top of the diamictite shows large 'flutes' or undulations (Figure 12) with the strike of the troughs parallel to the regional ice-flow direction.

Facies 4 (stratified, fine, clast-rich diamictite)

The facies which outcrops in the stream-bed, consists of fine, clast-rich diamictite alternating with mudrock units between 2 and 3 cm thick (Figure 7). The diamictite beds, which are up to 20 cm thick, consist of subrounded to angular dispersed (CPD = 15%) clasts of up to 10 cm in diameter in an argillaceous matrix (Figure 13). The stones show poor clast a-axis orientations with k-values of about 2 (Figure 5). The top of the main diamictite bed is arenaceous as part of the clay matrix was removed by water reworking (Figure 13).

The interbedded mudrocks consist of dark-grey silty shale with small amounts of dispersed angular granules and grains, thinly bedded clayey siltstone, and lonestone argillite (unit 3 in Figure 14). The shale commonly forms a blanket deposit over the underlying diamictite of facies 2A (Figure 8).

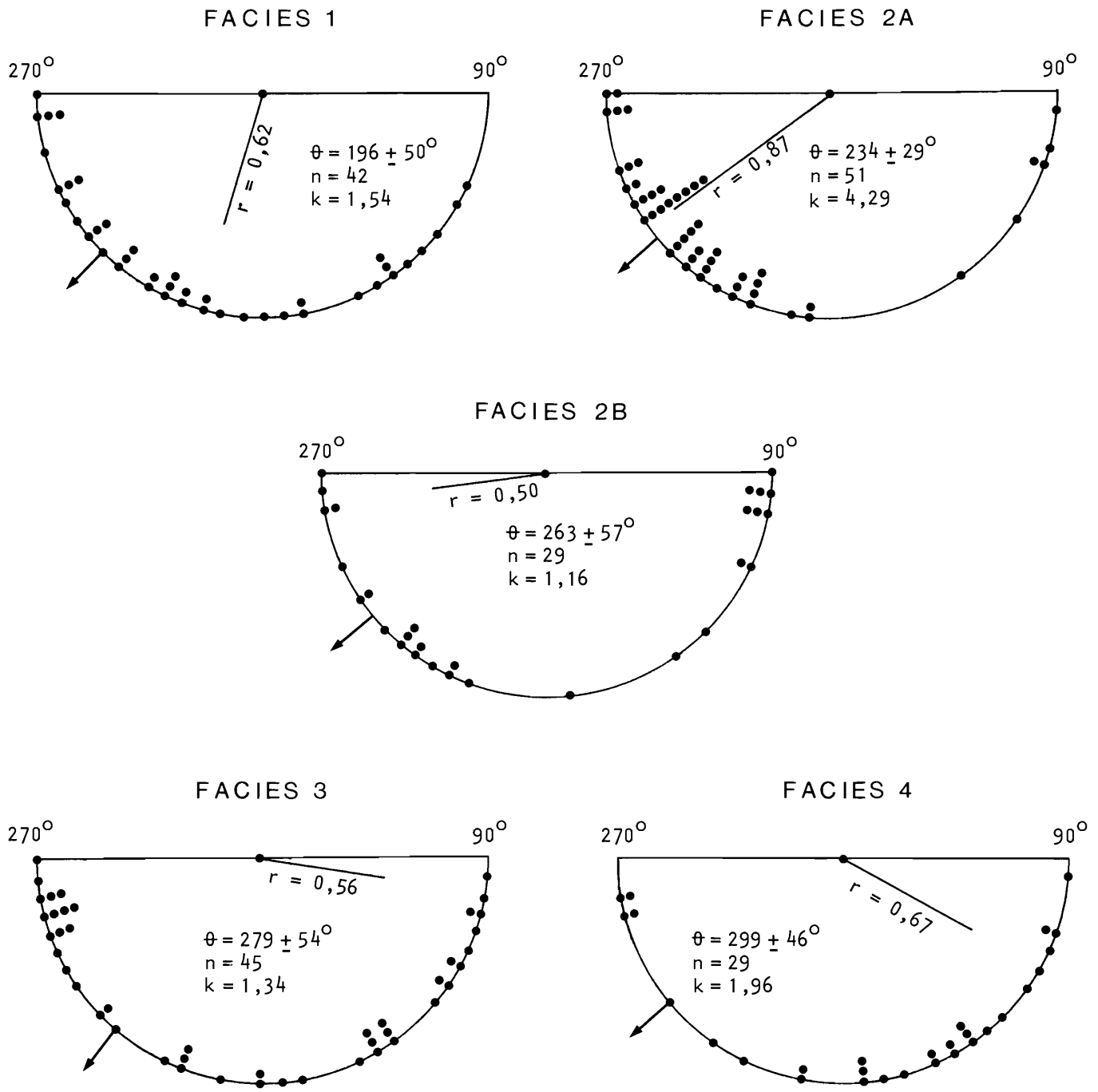

Figure 5 Representative fabric diagrams based on the Von Mises distribution (Till, 1974) of the four diamictite facies. General ice-flow directions indicated by arrows. θ = resultant clast a-axis orientation. n = number of readings. r = mean resultant length. k = concentration parameter.

Facies 5 (conglomerate)

The only exposure of this facies occurs on the western flank of pavement 3 where it varies from clast-supported boulder conglomerate (clasts up to 60 cm in diameter and little arenaceous to granular matrix) to small-pebble conglomerate (maximum clast size = 10 cm). In the latter type the clasts are partly matrix-supported (Figure 15). The clasts are rounded to subangular, generally poorly sorted, and in one sample, have a packing density of 44 per cent.

Facies 6 (mudrock)

The facies which forms a transitional contact with diamictite facies 4 (Figure 7), overlaps the diamictite at pavement 3 and west of the road where it directly overlies the Ventersdorp Supergroup bedrock. The mudrock sequence is up to 5 m thick (Slater, 1932), shows dips of up to 20° and consists of light to dark-grey carbonaceous shale with a few dispersed stones and granules. The stones, which are mostly rounded, are up to 75 cm in diameter in gullies next to the Vaal River. Thin diamictites are interbedded near the base of the facies, whereas thin interbedded brown ferruginous to calcareous siltstone beds, up to 25 cm thick, can be seen in the gullies. Lens-like carbonate to siliceous concretions are abundant. Although the shale in fresh

Figure 6 Leeside diamictite (facies 2B) filling an embayment with a bevelled edge at pavement 2. The side of the embayment is polished suggesting an older southward ice flow. Younger ice-flow direction indicated by an open arrow. Striae indicated by a solid arrow.

specimens resembles varves, thin section studies indicate the absence of grading (Slater, 1932), therefore the term 'rhythmite' is preferable.

Facies interpretation

The interpretation of the facies is based on the clast fabrics (k-values), the presence of bedding and water reworking, clast roundness and packing density, stratigraphic position of the facies in the inferred

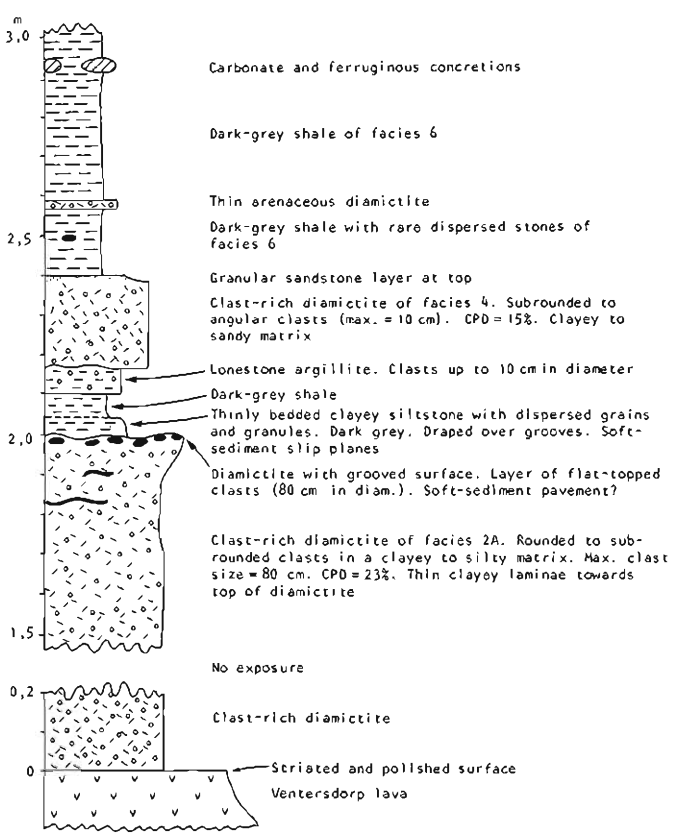

Figure 7 Stratigraphic section in stream-bed illustrating diamictite facies 2A and 4, and mudrock facies 6.

Figure 8 Mudstone with dispersed grains and granules draped over grooved diamictite of facies 2A (Dmt). Ice flow indicated by an open arrow.

Figure 9 Diamictite of facies 2B consisting of densely packed, rounded to subrounded clasts (CPD = 26%) in an argillaceous matrix. Pavement 2.

drumlinoid complexes, and the vertical facies relationships. The k-values for facies 1–4 are plotted as vertical bar scales in Figure 16 and, except for facies 2B and 3 which fall within the same range, a distinction between the facies can be drawn. The values were also compared with that of melt-out and debris-flow diamicton (Lawson, 1979), and lodgement diamicton (Dowdeswell & Sharp, 1986).

Facies 1 shows a low matrix content, a high density of rounded clasts, a very poor clast orientation, deposition along a median ridge on the leesides of bedrock knobs, and abrasion of the topmost clasts to form a possible boulder pavement. The deposition of leeside 'tails' can be attributed to subglacial cavity filling (Boulton, 1982a), plastic flow of diamicton (Boulton, 1976), erosion of diamicton (Moran *et al.*, 1980), or deposition by convergent ice streams on the leeside of obstructions (Moran *et al.*, 1980; Jones, 1982). As the bouldery diamictite occurs on bedrock and shows marked differences with other diamictites in the area, its formation by plastic flow, erosion, or deposition by convergent ice streams can be ruled out.

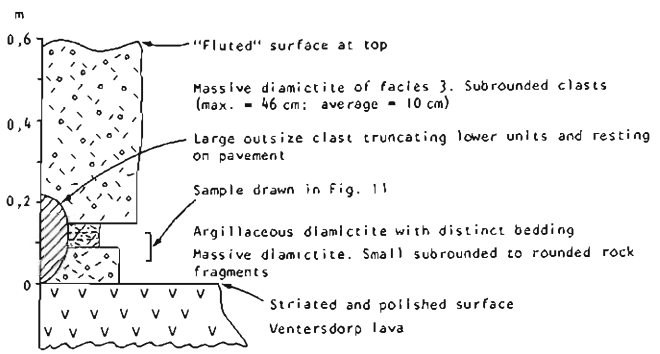

Figure 10 Stratigraphic section across diamictite facies 3 at pavement 2.

It is suggested that the bouldery diamictite was deposited in a subglacial leeside cavity by the expulsion of large stones from the sole of the glacier and subordinate basal melting (Figure 17). According to Boulton (1982a) large rocks, after being moved by the ice over an obstacle, can be extruded by the net force in the ice into the cavity. The shortage of matrix can be attributed to the partial removal of fine material by meltwater in the cavity and because the debris-laden basal ice lost part of its fine load on the stoss-side of the bedrock obstruction. Periodic closure of the cavity due to changes in the ice velocity caused the abrasion of the tops of the large clasts. The closure, however, could also have contributed to the deformation of the deposit which is reflected in the poor clast orientation. Dowdeswell & Sharp (1986) reported that where clast-clast contacts are frequent in basal debris-rich ice, fabric strength is also significantly reduced.

Facies 2A, which appears to be massive, contains about 75 per cent argillaceous matrix and shows a good clast orientation. It occurs in floor lows away from the bedrock knobs where the basal ice had been undeformed

Figure 12 Diamictite of facies 3 on stoss-side of pavement 2. Undulating ('fluted') top of the diamictite with troughs striking parallel to the regional ice-flow direction and soft-sediment veneer (short arrow) plastered onto pavement. Ice-flow direction indicated by a long arrow.

Figure 13 Diamictite of facies 4 consisting of dispersed, subrounded clasts (CPD = 15%) in an argillaceous matrix. Exposed in stream-bed. Top of bed (lighter coloured) more arenaceous and granular due to reworking by water.

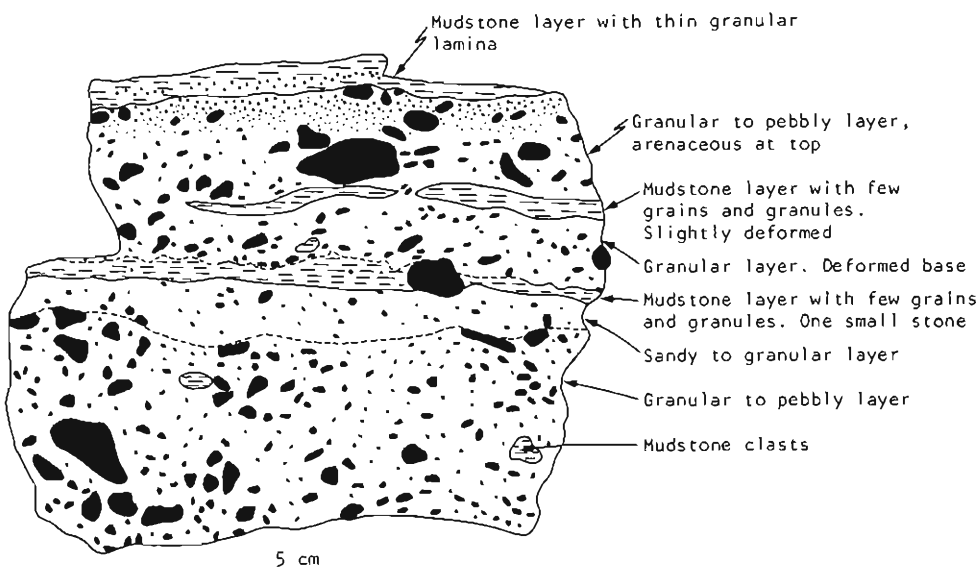

Figure 11 Detailed drawing of distinctly bedded diamictite of facies 3. Pavement 2.

Figure 14 Diamictite facies 4 in stream-bed. Unit 1 = thinly bedded argillaceous siltstone. Unit 2 = laminated silty shale. Unit 3 = lonestone argillite. Unit 4 = massive diamictite. The sequence formed by debris flow, rain-out from icebergs, and suspension settling from turbid plumes.

Figure 15 Conglomerate of facies 5 at pavement 3. It consists of densely packed, subrounded clasts (CPD = 44%) representing reworked diamicton.

resulting in a higher fabric strength (Boulton, 1971; Dowdeswell & Sharp, 1986), so that the observed clast orientation most probably reflects the original clast positions in the basal ice. The k-values of between 4 and 5 correspond the closest with that of lodgement diamicton (Figure 16) and a lodgement origin for the facies is therefore suggested. This conclusion is supported by the presence, on top of the deposit, of grooves which strike parallel to the regional ice-flow direction.

Facies 2B which has the same textural characteristics as facies 2A, except for the presence of a faint bedding in places and a very poor clast orientation, occurs in relatively small leeside embayments, where a lodgement origin can be ruled out. Deposition was either by strong melting of the basal ice forming the roof of a subglacial leeside cavity and the accumulation of the melt-out debris on the floor of the cavity (Boulton, 1982a), by the introduction of melt-out debris as a fine slurry into a subglacial leeside cavity (Boulton, 1982a), or by the *in situ* melt-out of debris- rich ice lodged in the cavity.

It is doubtful whether a slurry in such circumstances would have been able to transport stones up to 80 cm in diameter, whereas basal melt-out diamicton normally has extremely good clast a-axis orientations (Figure 16). Alternatively, strong melting of the ice roof of the cavity would have flushed out most of the fine material, but this is contrary to the matrix-supported character of the facies. The 30° difference between the clast orientation and the general ice-flow direction (Figure 5) suggests increasing deformation of either the basal debris-laden ice due to bedrock topography or the diamicton itself during overriding by the glacier. Thus it is possible that the facies could have been formed by the *in situ* melt-out of some basal ice accumulating in or becoming lodged in leeside cavities. The k-values are also similar to that of facies 3 (Figure 16) for which stronger evidence for an *in situ* melt-out origin exists. Haldorsen (1982) also described leeside melt-out diamicton in Åstadalen, Norway, which shows no strong preferred clast orientations.

Facies 3 with its generally smaller, subangular clasts, distinct small-scale bedding, diffused bed contacts, very poor clast orientation, sparse mudstone fragments, and a large deviation (45°) of clast long axes from the general ice-flow direction could have formed by the *in situ* melt-out of debris-rich ice, rain-out of debris from floating ice, or by sediment gravity flow. It is, however, doubtful whether waterlogged debris-rain or debris-flow deposits would have remained in position on such steep stoss slopes.

The diamictite shows on a small scale features typical of *in situ* melt-out diamicton (Lawson, 1981). The presence of out-size clasts that truncate layers are also described by Shaw (1982) in melt-out diamicton from the Edmonton area, Canada. It is therefore suggested that a sliver of the basal ice stagnated against the stoss-side of a bedrock knob (Figure 17) and slowly released its debris by melting (Boulton, 1982a; Eyles & Menzies, 1983). The very poor clast orientation of the facies would normally argue against a melt-out origin but case studies suggest that under certain circumstances, melt-out deposits could have poor clast fabrics. Shaw (1979) described basal melt-out diamicton in central Sweden that shows a weakly developed preferred clast orientation, which Shaw (1979) attributed to the little metamorphic foliation the debris-rich ice had experienced (described as poorly attenuated facies) before deposition. Boulton (1971) attributed abnormal clast fabrics in stoss-side diamicton on Svalbard to small-scale stress patterns in the basal ice caused by the configuration of the underlying bedrock topography. The same mechanism is suggested for the poor clast fabrics observed in the inferred melt-out diamictite of this facies. The undulating top of the facies at pavement 2 (Figure 12), interpreted in the past as a soft-sediment

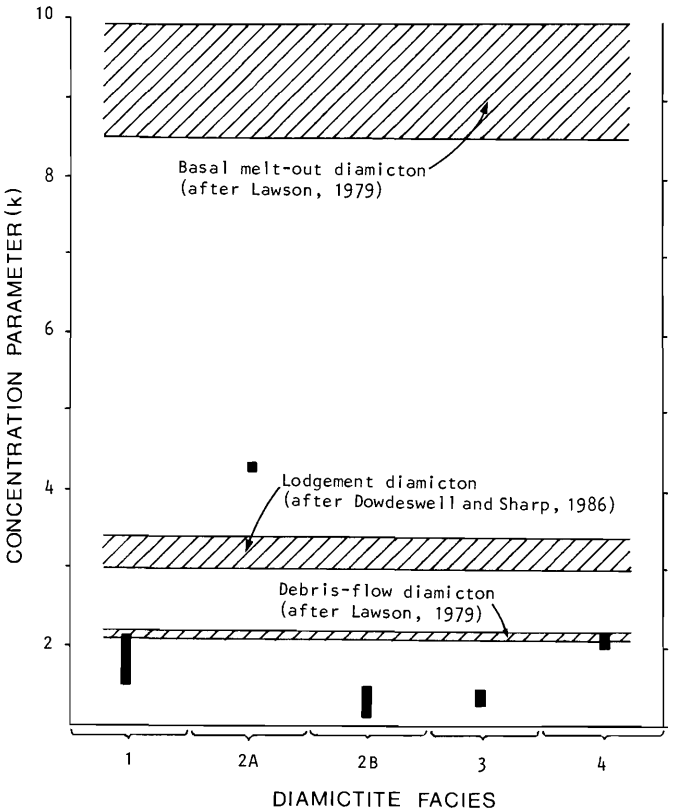

Figure 16 Plot of k-values (concentration parameter) as vertical bar scales for the diamictite facies. Fields for debris-flow, lodgement and basal melt-out diamicton are given for comparison.

pavement, could have formed during shear separating the stagnant basal ice from the overriding ice.

Facies 4 The stratification, interbedded mudrocks, small clasts, discrepancy between the clast long axis orientation and the general ice-flow direction, and the stratigraphic position of the facies towards the top of the diamictite sequence suggest a subaqueous debris-flow origin for the diamictite beds. The k-values for the facies also correspond well with that of debris-flow diamicton (Figure 16) described by Lawson (1979) at the Matanuska Glacier, Alaska. The diamictite beds probably formed as non-channelised lobes (Lawson, 1979) with a flow direction almost perpendicular to the general ice-flow trend (Figure 5). The arenaceous top of the major diamictite bed suggests reworking of the sediment by underflows debouching from the ice front. The interbedded mudrocks formed by suspension settling of mud supplied to the depository by possible overflows and minor rafting of debris by floating icebergs.

Facies 5 occurs in an area at pavement 3 where structures showing flow curvature are present (Figure 18). Similar features were interpreted by Shaw & Kvill (1984) as forms produced subglacially by running water (i.e. water sculptured erosion features). The lack of primary sedimentary structures and sandstone interbeds in the facies however argues against direct deposition of the coarse sediment by traction currents in subglacial tunnels. The facies is therefore interpreted as water-reworked diamicton which formed in subglacial tunnels along the flanks of bedrock knobs and in leeside cavities (Figure 17).

Facies 6, which consists of rhythmite shale, lonestone argillite, and interbedded thin diamictite and siltstone beds, formed by suspension settling of mud from turbid meltwater plumes, debris rain from icebergs, deposition by subaqueous debris flows, and fall-out from turbidity currents (McCabe, 1986). The rhythmites were deposited by silt-laden underflows debouching from the grounded ice front. The facies overlies debris-flow diamictite (facies 4), lodgement diamictite (facies 2A), melt-out diamictite (facies 3), and overlaps onto the basement which suggests that the area was rapidly inundated by a large water body. The ice front retreated in water so that all material was subsequently distributed by floating icebergs, subaqueous meltwater streams, and sediment gravity flow which led to the fine preservation of the basal diamicton facies in the area.

Implications for the glaciation model

The area comprising the Nooitgedacht pavements forms the southwestern margin of a large (18 km), glaciated, east-northeast-trending rock basin. The ice flowed about 30 m uphill out of the basin and this led to abnormal conditions at the base of the ice. This particular margin (remnant of an earlier glacial valley?) consists of irregular bedrock knobs which caused the ice to deform plastically with flow lines descending towards the bed and diverting around the flanks of the obstacles (Drewry, 1986). Although the uphill flow caused considerable frictional retardation on the basal sliding of the ice, this effect was reduced by the formation of subglacial cavities and water layers, which involved the decoupling of the ice from its bed (Eyles & Menzies, 1983). Another feature of the bedrock slope at Nooitgedacht is the asymmetrical step-like bedforms which can be seen to the southwest of pavements 2 and 3 (Figure 17). This can be attributed to low normal stresses at the base of the ice with the result that upglacier surfaces (stoss-sides) and the bases of leeslopes experienced substantial abrasion (Drewry, 1986).

The absence of lodgement diamicton covering the pavements (except for the thin veneer of finely abraded material plastered onto pavements, see Figure 12) indicates either a low debris concentration in the basal ice, or low effective stresses at the base of the ice (Boulton 1982a; Eyles & Menzies, 1983). The presence of leeside deposits suggests debris-rich basal ice so that low normal effective stress at the glacier bed resulted primarily in a bedrock swept clear of debris. This confirms the earlier conclusion on low normal stresses at the ice-bedrock interface during the formation of the step-like bedforms in the area.

The recognition of leeside diamictites (facies 1 and 2B) and the scarcity of plucking on the leeside of bedrock obstacles indicate the presence of leeside

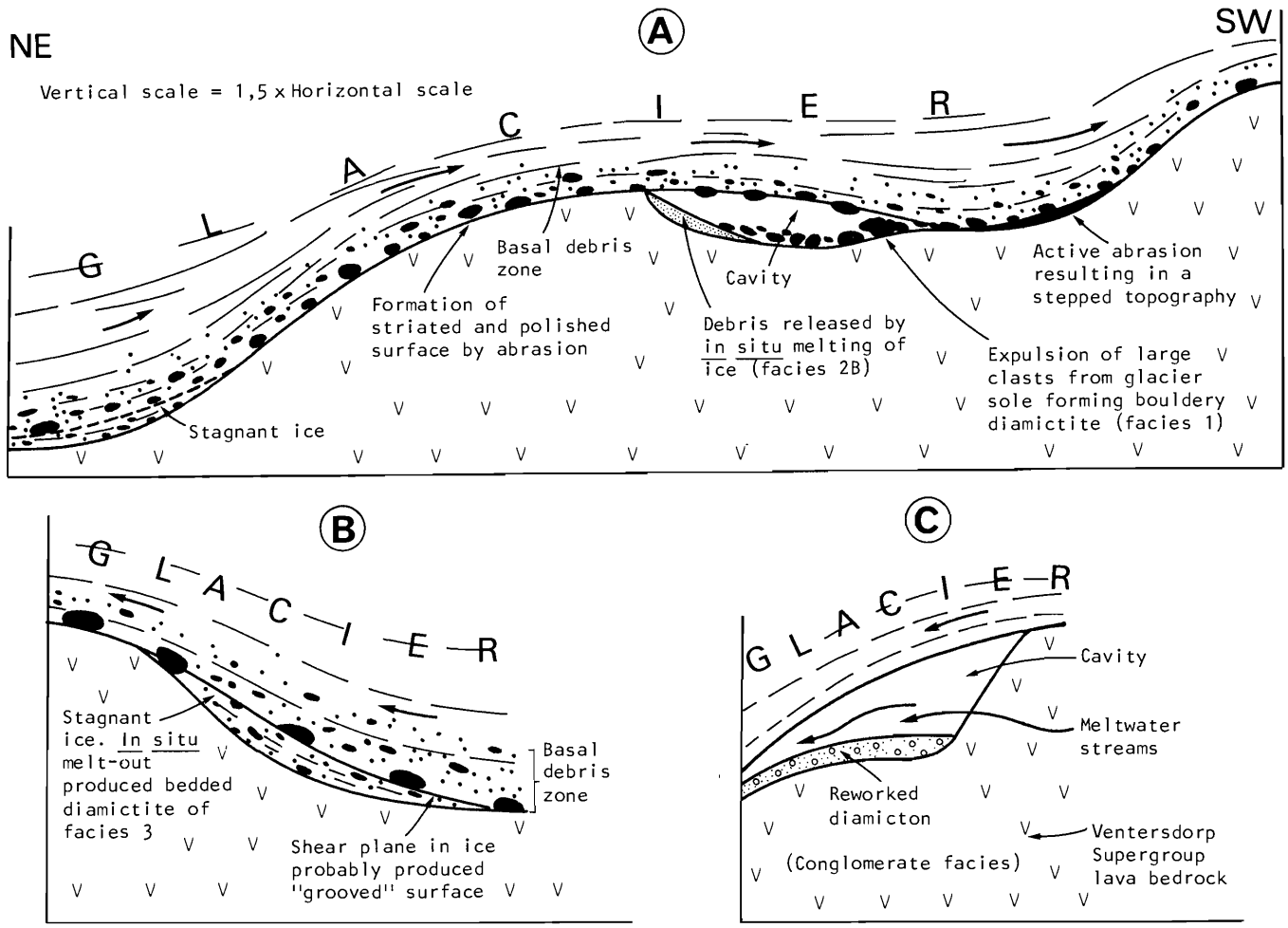

Figure 17 Depositional model. A – Deposition of bouldery diamictite facies 1 in a subglacial leeside cavity. B – *In situ* melt-out of stagnant debris-rich ice to produce facies 3 on stoss-side of bedrock obstruction. C – Formation of conglomerate facies 5 by the reworking of diamicton by meltwater streams in a subglacial tunnel/cavity.

cavities at the base of the glacier. Subglacial cavities develop where sliding velocity (v_i) is high, mean effective normal stresses (Nm) are low, and the aspect ratio (amplitude of obstruction divided by its length parallel to glacier flow) is high (Boulton, 1982a). Vivian & Bocquet (1973) described a 20 m long subglacial cavity at the base of the glacier d'Argentiére in France. The bedrock obstructions have an aspect ratio of 0,2 and the basal ice a sliding velocity of between 90 and 260 ma^{-1} which imply a mean effective normal stress of between 3,5 and 5 bars at the ice-bedrock interface. With increasing stress the cavities close and Boulton (1982a) calculated that with a v_i of 100 ma^{-1} and Nm > 6,5 bars no subice cavities will form. The mean effective normal stress is a function of the ice thickness and the water pressure on the ice-bedrock contact [$Nm = (p_i gh \times p_w)$ where p_i = ice density, g = gravitational acceleration, h = ice thickness, and pw = water pressure] (Boulton, 1982a). Therefore to reduce stress at the glacier bed, the ice must be thin and/or abundant meltwater must be present. This led to the general concept that leeside cavities develop and debris collects as subglacial scree in them during glacier retreat and ice thinning (Eyles & Menzies, 1983).

The problem of basal meltwater pressures has not yet been fully resolved. According to R. Le B. Hooke (pers. comm., 1987) water pressure depends largely on the influx of supraglacial meltwater through crevasses. Boulton (1982b) is of opinion that where ice moves over major obstructions and irregularities in its bed, the water layer is squeezed out from the ice-bedrock contact. The water pressure (p_w) is thus negligible, and Nm developed between the ice and the bedrock is undiminished. According to Weertman (1986) a water layer is always present at the ice-bedrock interface and that, in a steady state, the water pressure is close to the overburden ice pressure. Calculations, in the case of the glacier d'Argentiére, indicate that p_w lowered the Nm at the ice-bedrock interface by almost 50 per cent.

At Nooitgedacht there is little evidence of subglacial meltwater, except at pavement 3. As the lowest point of the rock basin was towards the west-northwest of the Nooitgedacht pavements, it can be assumed that most of the subglacial meltwater drained by means of tunnels in that direction. According to Weertman (1986) a flow of water through subglacial tunnels diminishes the water pressure, so that at Nooitgedacht, p_w at the ice-bedrock interface was apparently small. However, the ice front ended, at least during the final disintegration stage, in a

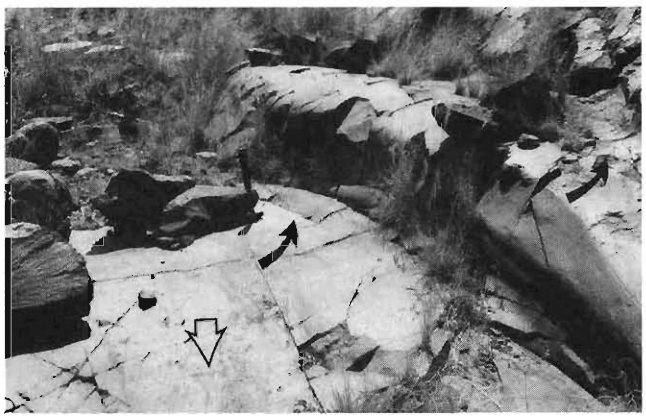

Figure 18 Water-sculptured erosion features showing evidence of flow curvature (solid arrows) at pavement 3. Ice-flow direction indicated by an open arrow.

water body which would have impeded the outflow of water through the subglacial tunnel system. As this would have resulted in less fluvially-eroded subglacial features and meltwater deposits, the volume of subglacial meltwater, as well as water-filled cavities, could have been underestimated. According to Dardis *et al.* (1984) an impeded outflow would also have enhanced cavitation. These conditions could have raised the values of p_w and thus diminished Nm at the glacier bed considerably.

At Nooitgedacht measurements of pavements 1 and 2 gave values of 0,17 for the aspect of the bedrock knobs. The maximum cavity lengths at pavements 1 and 2, judged from the length of the median ridges formed by facies 1, were about 30 m, but the boulder pavement suggests that towards the end of sedimentation the cavities were considerably smaller. The maintenance of the irregular topography at Nooitgedacht suggests a relatively low ice velocity, but with basal sliding sufficiently high for cavities to remain open. If a value for v_i of 200 to 300 ma^{-1} is assumed (using the maximum v_i at the glacier d'Argentiére as a norm), values for Nm of between 5 and 6 bars were obtained for conditions at the base of the glacier [after the graphs of Boulton (1982a)]. These are well within the limits for subglacial cavities to form, but imply an ice thickness of just over 50 m (assuming that the volume of subglacial meltwater was small and that outflow was not impeded at the ice front). This ice thickness figure is too low because, like the glacier d'Argentiére, widespread cavitation occurs beneath 150 m of ice (Vivian & Bocquet, 1973), and increased water pressures at the ice-bedrock interface must then be accepted. If these could have reduced Nm by at least 50 per cent, the ice thickness would be a 100 m or more, which would explain more readily the high degree of bedrock erosion at Nooitgedacht.

Boulton (1982b) stated that as a first approximation there is a linear increase in Nm on the bedrock with increasing ice thickness, from zero at the glacier snout to a maximum at the ice thickness where cavities are no longer found. During the period of formation of the drumlinoid complexes Nooitgedacht was probably located not far beyond the glacier snout and the area experienced the final deglaciation stage in the Karoo Basin. The almost abrupt change in deposition from subglacial diamictons to glaciolacustrine/glaciomarine sediments suggests a major inundation of the area and supplies additional evidence for a rapid, final destruction of the glaciers in the area.

The above-mentioned conclusions, however, do not imply that all the topographic features in the area formed during the final deglaciation stage. Engelbrecht (1973) stated that the oldest ice-flow direction was towards the south (170°/177°). The authors' measurements of the strike along a bevelled edge demarcating a leeside cavity at pavement 2 (Figure 6), indicate an older ice-flow direction of 155°. The last glacial episode that deposited the diamictites, conglomerate, and mudrocks therefore appears to have clearly modified existing glacial erosion structures at Nooitgedacht.

Acknowledgements

The authors are grateful to the FRD of the Council for Scientific and Industrial Research for the financial support given to this research.

References

Boulton, G.S. (1971). Till genesis and fabric in Svalbard, Spitsbergen. *In*: Goldthwait, R.P. Ed., *Till: a Symposium*. Ohio State University Press, Columbus, 41–72.

---- (1976). The origin of glacially fluted surfaces – observations and theory. *J. Glaciol.*, **17**, 287–309.

---- (1982a). Subglacial processes and the development of glacial bedforms. *In*: Davidson-Arnott, R., Nickling, W. & Fahey, B.D. Eds., *Research in Glacial, Glacio-fluvial, and Glacio-lacustrine Systems*. Geo Books, Norwich, 1–31.

---- (1982b). Processes and patterns of glacial erosion. *In*: Coats, D. R. Ed., *Glacial Geomorphology*. George Allen & Unwin, London, 41–87.

Dardis, G.F., McCabe, A.M. & Mitchell, W.I. (1984). Characteristics and origins of lee-side stratification sequences in late-Pleistocene drumlins, Northern Ireland. *Earth Surf. Process. Landf.*, **9**, 409–424.

Dowdeswell, J.A. & Sharp, M. (1986). Characterization of pebble fabrics in modern terrestrial glacigenic sediments. *Sedimentology*, **33**, 699–710.

Drewry, D. (1986). *Glacial Geologic Processes*. Edward Arnold, London. 276 pp.

Du Toit, A.L. (1906). Geological survey of the eastern portion of Griqualand West. *Ann. Rep. Geol. Comm. C. G. H.* for 1906, **11**, 87–176.

Engelbrecht, L.N.J. (1973). *Die Geologie van die Gebied Tussen Kimberley en Barkly-Wes, Kaapprovinsie*. M.Sc. Thesis (unpubl.), Univ. Orange Free State., Bloemfontein. 105 pp.

Eyles, N. & Menzies, J. (1983). The subglacial landsystem. *In*: Eyles, N. Ed., *Glacial Geology*. Pergamon Press, New York, 19–70.

Haldorsen, S. (1982). The genesis of tills from Åstadalen, southeastern Norway. *Norsk Geologisk Tidsskr.*, **62**, 17–38.

Jones, N. (1982). The formation of glacial flutings in east-central Alberta. In: Davidson-Arnott, R., Nickling, W. & Fahey, B.D. Eds., *Research in Glacial, Glacio-fluvial, and Glacio-lacustrine Systems*. Geo Books, Norwich, 49–70.

Lawson, D. E. (1979). Sedimentological analysis of the western terminus region of the Matanuska Glacier, Alaska. *CRREL Rep.*, **79–9**, 112 pp.

---- (1981). Distinguishing characteristics of diamictons at the margin of the Matanuska Glacier, Alaska. *Ann. Glaciol.*, **2**, 78–84.

McCabe, A.M. (1986). Glaciomarine facies deposited by retreating tidewater glaciers. An example from the late-Pleistocene of Northern Ireland. *J. sedim. Petrol.*, **56**, 880–894.

Moran, S.R., Clayton, L., Hooke, R. Le B., Fenton, M. M. & Andriashek, L.D. (1980). Glacier-bed landforms of the prairie region of North America. *J. Glaciol.*, **25**, 457–476.

Shaw, J. (1979). Genesis of the Sveg tills and Rogen moraines of Central Sweden: a model of basal melt out. *Boreas*, **8**, 409–426.

---- (1982). Forms associated with boulders in melt-out till. *In*: Evenson, E.B., Schlüchter, Ch. & Rabassa, J. Eds., *Tills and Related Deposits*. A. A. Balkema, Rotterdam, 3–12.

Shaw, J. & Kvill, D. (1984). A glaciofluvial origin for drumlins of the Livingstone Lake area, Saskatchewan. *Can. J. Earth Sci.*, **21**, 1442–1459.

Slater, G. (1932). The glaciated surfaces of Nooitgedacht, near Kimberley, and the Upper Dwyka boulder shales of the eastern part of Griqualand West (Cape Province), 1929. *Trans. roy. Soc. S. Afr.*, **20**, 301–325.

Stratten, T. (1968). *The Dwyka glaciation and its relationship to the Pre-Karroo Surface*. Ph.D. Thesis (unpubl.), Univ. Witwatersrand, Johannesburg. 196 pp.

Till, R. (1974). *Statistical Methods for the Earth Scientist*. MacMillan, London. 154 pp.

Vivian, R.A. & Bocquet, G. (1973). Subglacial cavitation phenomena under the glacier d'Argentiére, Mont Blanc, France. *J. Glaciol.*, **12**, 439–451.

Weertman, J. (1986). Basal water and high pressure basal ice. *J. Glaciol.*, **32**, 455–463.